"Viable Motheaten," a New Allele at the Motheaten Locus

I. Pathology

LEONARD D. SHULTZ, PhD,
DALE REX COMAN, MD, CHERYL L. BAILEY,
WESLEY G. BEAMER, PhD, and
CHARLES L. SIDMAN, PhD

From The Jackson Laboratory, Bar Harbor, Maine

A new spontaneous autosomal recessive mutation has recently occurred at the motheaten *(me)* locus on Chromosome 6 in strain C57BL/6J mice. Homozygotes for the new allele, designated "viable motheaten" (me^v), have a mean life span of 61 ± 2.4 days, compared with only 22 ± 1.3 days for C57BL/6J-*me/me* mice. Like the original motheaten mutation, the immediate cause of death in me^v/me^v mice appears to be severe pneumonitis associated with accumulations of macrophages, granulocytes, and lymphocytes in the lungs. However, because of its longer life span, progression of the disease in me^v/me^v mice is more amenable to investigation. Eosinophilic crystalline material in alveolar macrophages from me^v/me^v mice is associated with extravasation of erythrocytes into alveoli. These crystals are morphologically indistinguishable from hematoidin, which results from hemoglobin breakdown following uptake of erythrocytes by macrophages. Severe macrocytic hypochromic anemia with abnormalities in size and shape of erythrocytes develops by 7 weeks. A twofold increase in peripheral leukocyte count and a fivefold increase in the percentage of neutrophils is seen by 10 weeks. Viable motheaten mice develop focal granulocytic skin lesions by 4 days of age, show depletion of cells from the thymus cortex by 4 weeks, and lack lymphoid follicles in the lymph nodes, spleen, and Peyer's patches. Excessive erythropoiesis and myelopoiesis in the spleen result in marked splenomegaly. Lymph nodes and spleens from me^v/me^v mice contain increased numbers of plasma cells by 3 weeks; and by 6 weeks, large numbers of atypical plasma cells with Russell bodies are evident. Development of glomerulonephritis by 10 weeks is characterized by granular deposits of immunoglobulin and complement within glomeruli. A twofold increase of blood urea nitrogen levels is present by 15 weeks. Sterility of male me^v/me^v mice is associated with Leydig cell depletion in the testes, lowered testosterone levels, and impaired spermatogenesis. (Am J Pathol 1984, 116:179–192)

RESEARCH on the underlying mechanisms of genetically determined immunologic disease has benefited by the discovery of new murine single gene mutations that cause defects in the development or regulation of the immune system.[1,2] The most deleterious of the currently known immunologic mutations is the autosomal recessive "motheaten" (*me*). Despite a severe functional deficiency of T-lymphocytes, B-lymphocytes, and natural killer (NK) cells,[3–6] homozygotes (*me/me*) produce abnormally high levels of circulating immunoglobulins and express autoantibodies against thymocytes and double-stranded DNA.[3,7] Determination of the basis for the faulty regulation of the immune system in motheaten mice would contribute to our understanding of complex genetically determined immunologic diseases in man. However, investigations with this mutant are restricted because even the longest lived homozygotes (*me/me*) die by 6 weeks of age from a pneumonitis of unknown etiology.[8]

A new spontaneous autosomal recessive mutation appeared in 1980 in C57BL/6J mice at the Jackson Laboratory. Homozygotes developed focal abscesses on the surface of the skin by 4 days of age, and grew slowly during a maximum life span of 25 weeks. Allelism tests between mice heterozygous for the new mutation and obligate heterozygotes (+/*me*) for the

Supported by Grants CA-20408, CA-24145, CA-35845, CA-34196 and AI-20232 from the United States Public Health Service.

The Jackson Laboratory is fully accredited by the American Association for Accreditation of Laboratory Animal Care.

Accepted for publication February 8, 1984.

Address reprint requests to Leonard D. Shultz, The Jackson Laboratory, Bar Harbor, ME 04609.

motheaten mutation showed the new mutation to be an allele of *me* on Chromosome 6. Since homozygotes for the new mutation survived longer than C57BL/6J-*me/me* mice, the new allele was designated "viable motheaten" (*me^v*). This report describes the pathologic effects of the viable motheaten mutation.

Materials and Methods

Mice

Viable motheaten mice used in this study were from the C57BL/6J-*me^v* strain propagated by +/*me^v* brother/sister matings. Littermate controls consisted of approximately two-thirds +/*me^v* and one-third +/+, the two genotypes being indistinguishable. Motheaten mice used for comparison of life span and pathologic effects were from the C57BL/6J-*me* strain. The original *me* mutation occurred in the C57BL/6J strain.[8] To reduce the possibility of subline divergence, there have been nine generations of backcrosses to C57BL/6J, accomplished by transplanting ovaries of *me/me* females to histocompatible hosts and mating to C57BL/6J males. All mice were fed a standard diet of Old Guilford Number 96 pelleted food (Emery Morse Co., Guilford, CT) and received chlorinated water *ad libitum.*

Histopathology

Tissues for histologic examination were fixed in Fekete's formol-acetic alcohol,[9] embedded in paraffin, and sectioned at 8 μ. Selected tissues were fixed as described for electron microscopy, embedded in JB4 plastic, and sectioned at 2 μ. Slides were stained with Mayer's hematoxylin and eosin (H&E), periodic acid–Schiff (PAS) reagent, methyl green/pyronin, and Gomori's iron stain.

Immunofluorescence

Determination of immunoglobulin and complement deposition in 8-μ frozen sections of tissues from *me^v/me^v* and littermate control mice was carried out as previously described.[3] Fluorescein-conjugated polyspecific goat antibodies against total mouse Ig (heavy plus light chain), as well as heavy chain specific antisera againt IgG, IgM, and IgA and antisera against mouse C3 (Cappel), were absorbed with mouse liver powder (Cappel) and spun at 100,000*g* for 30 minutes immediately before use. Sections were examined in a Leitz Orthoplan microscope equipped for epifluorescence. Pictures were taken with Kodak Tri-X Pan film (ASA 400).

Electron Microscopy

Lymphoid tissues were fixed in 2% glutaraldehyde, 1% paraformaldehyde in 0.1 M cacodylate buffer, pH 7.4. The tissues were then postfixed in 1% osmium tetroxide, stained in block with 0.5% uranyl acetate, dehydrated, and embedded in Epon–araldite. Ultrathin sections were stained again with uranyl acetate followed with lead citrate, then viewed in a Hitachi 11-C electron microscope operated at 75 kv.

Hematology

Blood was collected with heparinized capillary tubes from either the retroorbital sinus in mice over 2 weeks of age, or from the superficial temporal vein in younger mice. Erythrocytes were counted by standard techniques with a model ZBI Coulter Counter. Erythrocyte mean corpuscular volumes (MCVs) were calculated from the packed red cell volumes and counts as described elsewhere.[10] Mean corpuscular hemoglobin concentration (MCHC) was assayed by the cyanohemoglobin technique.[11]

Blood smears for reticulocyte counts were prepared after mixing two parts of fresh heparinized blood with one part of 1% brilliant cresyl blue in isotonic saline. Counts of total white blood cells were made in counting chambers after dilution in 2% acetic acid with 0.01% crystal violet. Smears for differential counts were stained with May–Grünwald Giemsa. At least 300 randomly chosen white blood cells were classified according to Dunn's criteria.[12] Histochemical localization of myeloperoxidase and chloroacid esterase was carried out as previously described.[13]

Blood Urea Nitrogen

Serum blood urea nitrogen (BUN) values were determined with the use of a colorimetric assay (Pierce Chemical Company, Rockford, IL). Each assay included commercial standards with 10–120 mg/dl urea.

Quantitation of Testosterone

Plasma testosterone levels were estimated by radioimmunoassay utilizing a rabbit anti-testosterone antibody (number 1720; Radioassay Systems Laboratory Inc., Carson, CA) able to detect 0.04 ng/ml testosterone in plasma. The antibody crossreacts approximately 19% with dihydrotestosterone, a steroid me-

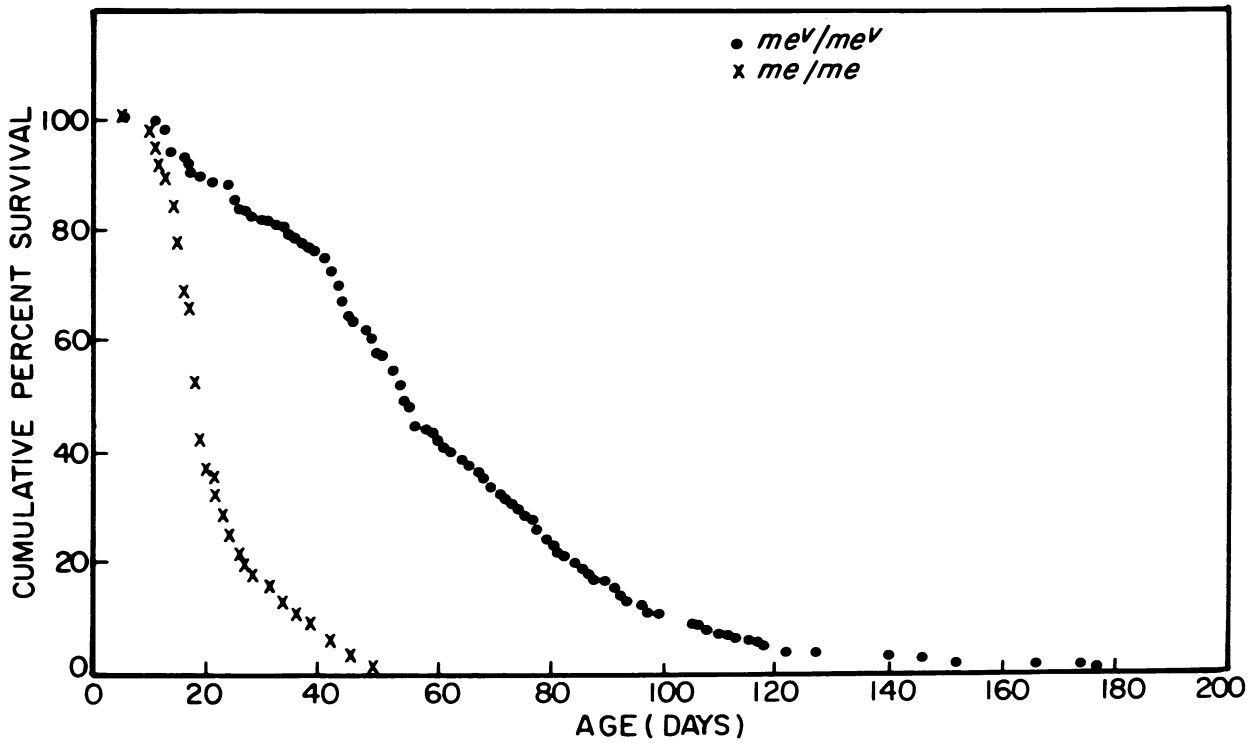

Figure 1 — Cumulative percent survival of *me/me* and *me^v/me^v* mice. Data are based on 57 *me/me* and 180 *me^v/me^v* mice. The littermate control mice for both mutations show greater than 95% survival at 1 year of age.

tabolite not present in significant concentration in mouse blood.[14] Steroids in plasma samples (0.1 ml) were extracted with 5 ml anhydrous diethyl ether, and then the organic solvent phase was separated and dried under N_2 gas. Dried extracts were resolubilized in phosphate-buffered saline containing 1% gelatin and assayed in duplicate. Testosterone values were corrected for volume extracted and methodologic recovery, then expressed as nanograms of testosterone per milliliter of plasma.

Statistical Analysis

All measures of variance are given as standard errors of the mean. Tests of significance for differences between independent means were performed with the Student *t* test or one-way analysis of variance.

Results

Longevity

To determine the longevity of *me^v/me^v* mice, 97 male and 83 female homozygotes were observed from 4 days of age until death. There was no significant effect of sex on the survival of this mutant. The mean life span of these 180 *me^v/me^v* mice was 61 ± 2.4 days. This is in contrast to the comparatively short longevity of C57BL/6J-*me/me* mice. The mean life span of 57 *me/me* mice (27 female and 30 male) was 22 ± 1.3 days. As with *me^v/me^v* mice, there was no effect of sex on longevity. Figure 1 shows the cumulative percent survival of *me/me* and *me^v/me^v* mice. Compound *me/me^v* mice generated from mating known heterozygotes (+/*me* × +/*me^v*) survived for a mean of 65 ± 7.2 days, indicating that with respect to longevity the *me^v* allele is dominant to the *me* allele.

Peripheral Blood Counts

From 3 to 6 weeks of age, *me^v/me^v* mice have normal erythrocyte counts, but anemia becomes evident by 7 weeks (Figure 2a). After 10 weeks, erythrocyte levels fall to 50% of those seen in age-matched littermate control mice. An increase in erythrocyte mean cell volume (MCV) develops concomitantly with anemia in this mutant. While the erythrocyte MCV of littermate control mice remains relatively constant between 3 and 24 weeks of age, the erythrocyte MCV of *me^v/me^v* mice is significantly elevated by 7 weeks and

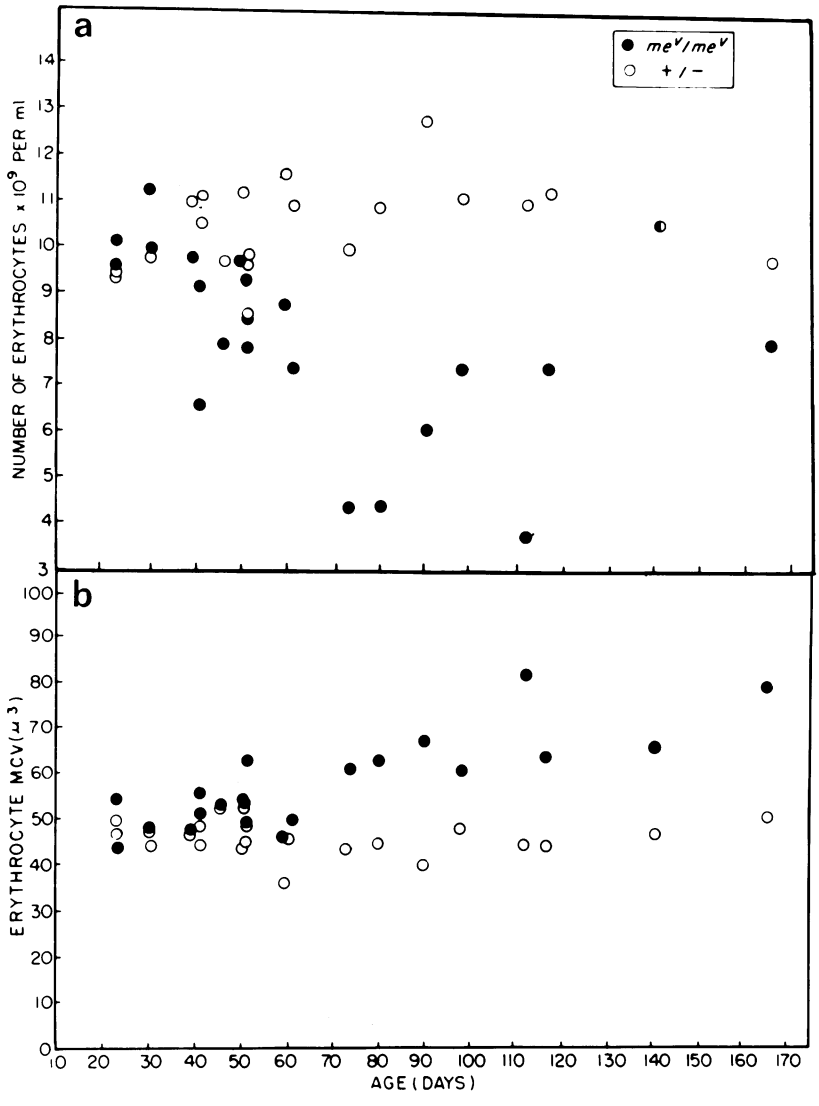

Figure 2—Erythrocyte counts and mean cell volumes from individual me^v/me^v mice and littermate +/− controls.

thereafter throughout the life span of this mutant (Figure 2b). Analysis of reticulocyte levels showed a fourfold increase in the percentage of reticulocytes in me^v/me^v mice, compared with those in littermate control mice. Comparison of ten pairs of me^v/me^v and littermate control mice at 4–9 weeks of age showed a reticulocyte count of 15.2% ± 1.56% for me^v/me^v mice versus 3.8% ± 0.36% for +/− controls ($P < 0.01$).

Examination of blood smears from me^v/me^v mice showed abnormalities in size, shape, and staining characteristics of erythrocytes by 3 weeks of age. These abnormalities became progressively more severe with age. By 15 weeks there was marked anisocytosis and polychromasia (Figure 3). Since many of the erythrocytes observed in blood smears from me^v/me^v mice were pale, we determined hemoglobin levels. There was a 10% decrease in mean corpuscular hemoglobin concentration (MCHC) in me^v/me^v mice after 5 weeks of age. The mean MCHC for 4 me^v/me^v mice aged 6–11 weeks was 30.1 ± 0.23, compared with 33.1 ± 0.35 for age-matched littermate control mice ($P < 0.05$).

Viable motheaten mice had normal peripheral leukocyte counts until 7 weeks of age, but by 10 weeks there was a twofold increase in the number of circulating white blood cells. The mean white cell count for 9 me^v/me^v mice aged 9–24 weeks was 22.5 ± 4.39 × 10^6/ml, compared with 9.9 ± 0.95 × 10^6/ml for age-matched littermate control mice ($P < 0.05$). At all ages tested, differential counts showed a twofold decrease in the percentage of lymphocytes and a fivefold increase in the percentage of neutrophils. The mean percentage of circulating lymphocytes for 10

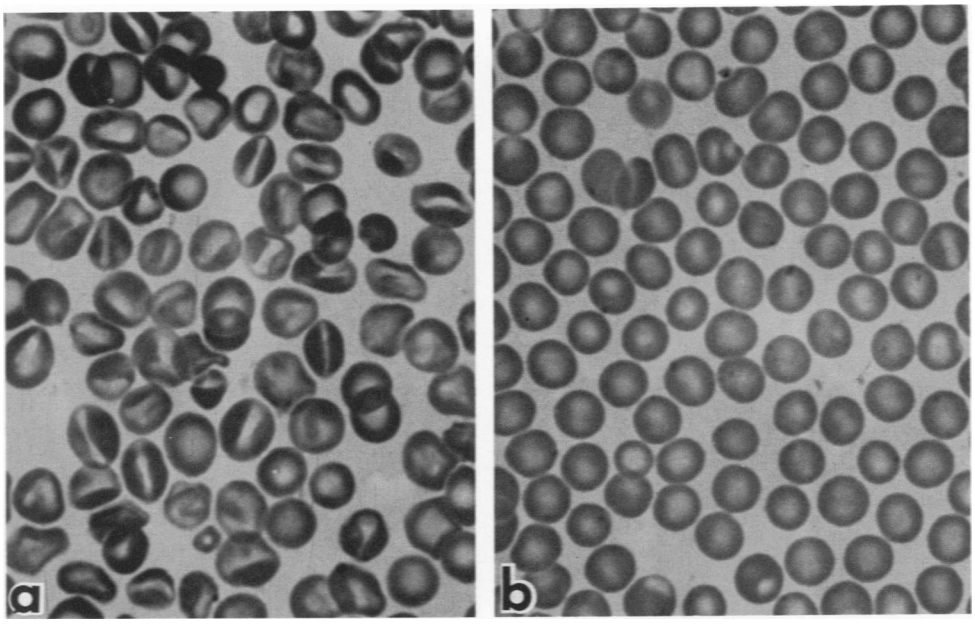

Figure 3 – Blood smears from 15-week-old mice. **a** – *me^v/me^v* mouse showing variations in shape and size of erythrocytes. **b** – Littermate +/– control mouse with normal erythrocytes. (May-Grünwald Giemsa, ×750)

me^v/me^v mice aged 4–16 weeks was 34.9% ± 4.26%, compared with 84.3% ± 1.44% for age-matched littermate control mice. The mean percentage of circulating neutrophils for these mice was 58.9% ± 3.74% in *me^v/me^v* mice, compared with 11.6% ± 1.43% for littermate control mice. While most of the neutrophils examined in blood smears from littermate control mice appeared to be relatively mature as judged by the multilobular appearance of their nuclei, the majority of neutrophils in blood smears from viable motheaten mice were immature, having spherical or early ring-form nuclei containing finely divided chromatin. To identify the immature granulocytes more reliably, blood smears from six pairs of *me^v/me^v* and +/– littermate control mice were stained for the presence of chloroacid esterase and myeloperoxidase. Since the immature granulocytes stained strongly for both enzymes, their myeloid lineage was verified.

Histopathology

Tissues for histologic analysis were removed from 21 pairs of viable motheaten and littermate control mice from 4 to 166 days after birth. Homozygous *me^v/me^v* mice developed focal subdermal accumulations of neutrophils, resulting in patchy loss of pigment and irregular hair growth.

As observed in *me/me* mice, *me^v/me^v* homozygotes develop an unusual pneumonia. However, the lung lesions progress more slowly in the *me^v/me^v* mice. By 10 weeks of age, large numbers of macrophages are evident within the alveoli of *me^v/me^v* mice. These macrophages frequently contain fine nonbirefringent crystalline material and occasional erythrocytes. Larger needlelike crystals also appear within macrophages, and coarse crystals are seen lying free outside of cells (Figure 4). Although such crystalline material has been previously described in lungs of *me/me* mice, its nature and its role in the spontaneous pulmonary lesions have not been determined. The deposition of large amounts of hemosiderin within alveolar macrophages of *me^v/me^v* mice suggests that the presence of crystalline material may be associated with erythrocyte degradation. Sections of lung incubated with Gomori's iron stain revealed large amounts of hemosiderin within macrophages. Although the crystals themselves did not stain for iron, they were usually associated with hemosiderin deposits. In *me^v/me^v* mice that survived to 20 weeks of age, pneumonia affected all lobes of the lung, and erythrocytes were evident free in the alveoli as well as within macrophages.

In *me^v/me^v* mice the thymus appears histologically normal at 1–3 weeks of age but shows cortical depletion by 4 weeks (Figure 5). A decrease in thymus size is evident by 4 weeks, and by 16 weeks nothing recognizable as a thymus is seen in the mediastinal area of this mutant (Figure 6a). In contrast to the decreased thymic cellularity, the spleen increases greatly in size from birth onward (Figure 6b). At 16 weeks of age,

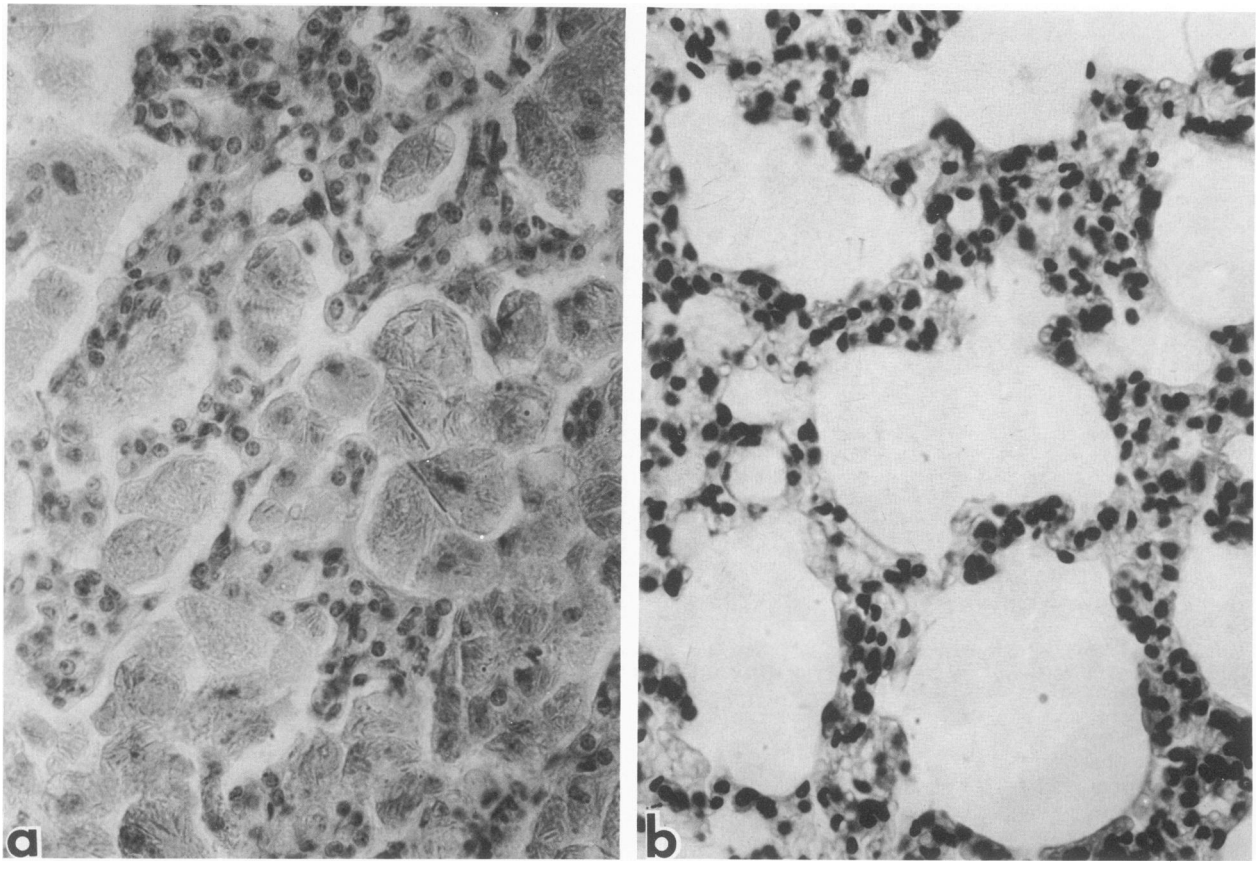

Figure 4—Lungs from 10-week-old mice. **a**—*me^v/me^v* lung showing accumulations of macrophages within alveoli. Crystalline inclusions are seen within macrophages. **b**—Littermate +/− lung showing normal structure. (H&E, ×300)

the spleen/body weight ratio in *me^v/me^v* mice is tenfold higher than that in littermate control mice. Splenomegaly results from increased erythropoiesis and myelopoiesis. Histologic examination of spleens from *me^v/me^v* mice shows depletion of lymphocytes from the periarteriolar regions by 1 week of age and severe depletion of the white pulp by 15 weeks (Figure 7). In contrast to the spleen, the bone marrow of *me^v/me^v* mice, shows diminished erythropoiesis and increased myelopoiesis. Lymph nodes and Peyer's patches from *me^v/me^v* mice lack cortical follicles and show a decreased density of lymphocytes throughout, compared with those of littermate control mice. Multinucleated giant cells are scattered throughout lymph nodes from *me^v/me^v* mice, and larger numbers of plasma cells and neutrophils are evident, especially in the sinuses. Interspersed with the plasma cells in lymph nodes and spleens of *me^v/me^v* mice, but not control mice, were atypical plasma cells containing discrete PAS-positive inclusions (Figure 8). Such cytoplasmic inclusions have been referred to as "Russell bodies."[15] They appear in plasma cells by the fourth week of age and increase in number throughout the life span of *me^v/me^v* mice. Plasma cells with Russell bodies were also found scattered throughout the lungs of this mutant. Electron-microscopic examination of lymph nodes from *me^v/me^v* mice showed many atypical plasma cells with osmophilic globules located within the cisternae of rough endoplasmic reticulum (Figure 9). These plasma cells were often of irregular shape and Russell-body–containing cells with pseudopodial extensions were not uncommon.

Kidneys from viable motheaten mice showed hypercellularity of the glomeruli by 10 weeks of age. By 20 weeks, these mice developed marked glomerulonephritis (Figure 10). PAS-positive material was evident within glomeruli and in tubules. Immunofluorescence analysis of frozen kidney sections from five *me^v/me^v* mice tested at 10 weeks of age showed granular deposits of IgM, IgG, and C3 within glomeruli (Figure 11a). Kidneys from littermate control mice were either negative for immunoglobulin and C3 deposits or showed only slight reactivity in a few scattered glomeruli after incubation with anti-IgM antibody. Ele-

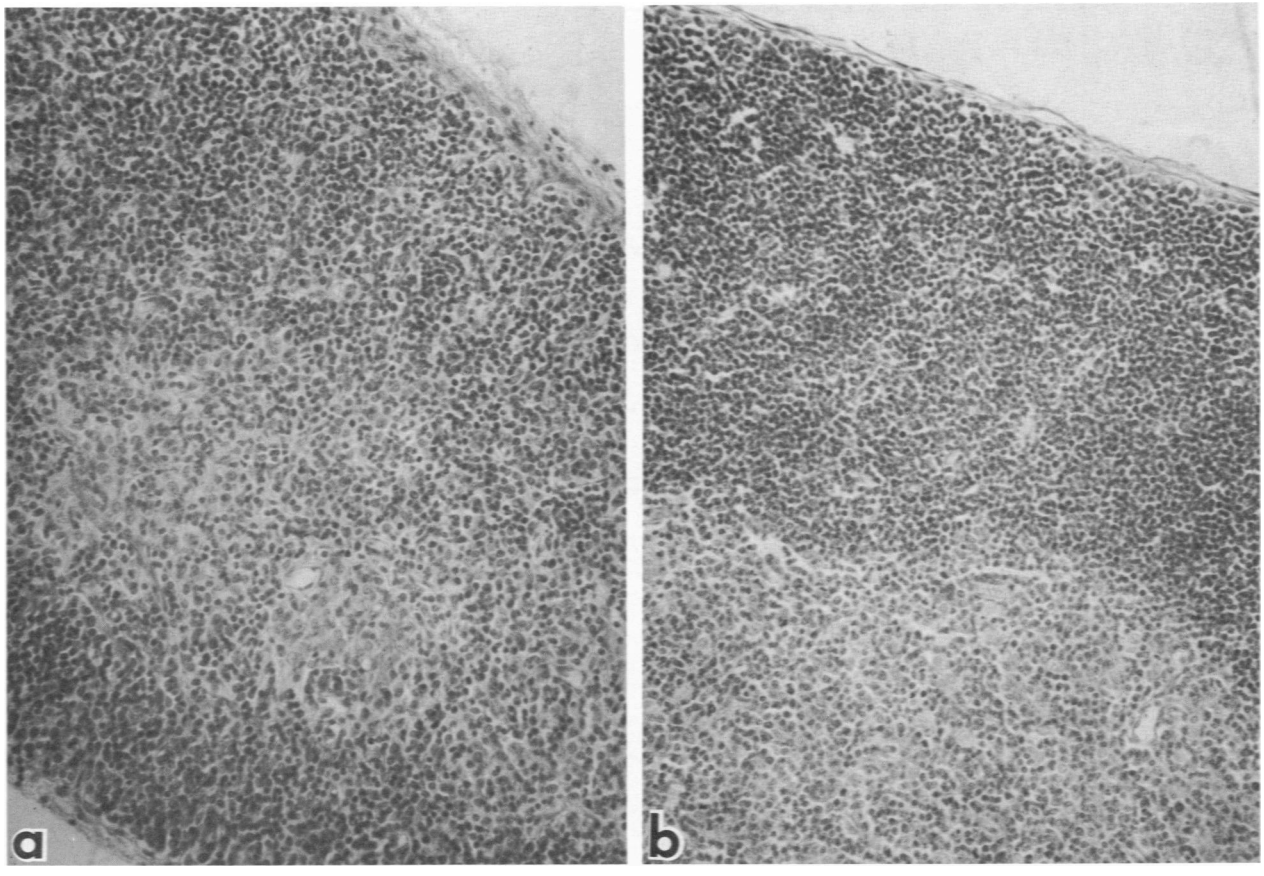

Figure 5—Thymuses from 4-week-old mice. **a**—*me^v/me^v* thymus showing depletion of cells from the cortex. **b**—Littermate +/− thymus showing normal structure. (H&E, × 150)

vated levels of BUN indicated that kidneys from *me^v/me^v* mice did not function properly. Quantitation of BUN in sera from 21 pairs of *me^v/me^v* and +/− littermate mice at 1 to 5 months of age showed a significant increase ($P < 0.05$) in BUN of *me^v/me^v* mice at 4–5 months. The mean level of BUN for 9 pairs of mice at 15–22 weeks of age was 83.1 ± 19.17 mg/dl for *me^v/me^v* mice versus 35.2 ± 2.75 mg/dl for +/− controls.

In addition to Ig in the kidneys, we also found such deposits in the skin, thymus, lungs, and testes of *me^v/me^v* mice. As shown in Figure 11b, the lungs of *me^v/me^v* mice had conspicuous accumulations of IgM around arterioles. Phase-contrast microscopy showed mononuclear cell infiltrates in association with the Ig deposits. Similar tissues from littermate control mice were negative for Ig deposition.

Although viable motheaten mice survive up to 25 weeks of age, we were unable to propagate these mice by homozygous matings. Female and male *me^v/me^v* mice are sterile; no offspring resulted from numerous matings between *me^v/me^v* females and +/− males or between *me^v/me^v* males and +/− females. Ovaries from *me^v/me^v* mice aged 10–14 weeks contained normal-appearing and variably sized oocytes. Follicular structures ranged from a single layer of granulosa cells surrounding oocytes to large numbers of such cells and initial cavity formation typical of follicles in young littermate control mice. Neither corpora lutea nor corpora albicans, indicative of ovulatory activity, were observed, however. Transplantation of homozygous mutant (*me^v/me^v*) ovaries into histocompatible ovariectomized normal hosts, followed by mating with C57BL/6J +/+ males, resulted in live offspring genetically derived from donor ovaries.

Testes from *me^v/me^v* mice appeared abnormal by 2 weeks of age. Infiltration of neutrophils between testicular tubules was observed at 11 days. By 4 weeks, the number of interstitial Leydig cells was reduced. Within testicular tubules of 10-week-old *me^v/me^v* mice, spermatogenesis was arrested at the secondary spermatocyte stage; consequently, no mature sperm were produced (Figure 12). Since spermatogenesis is

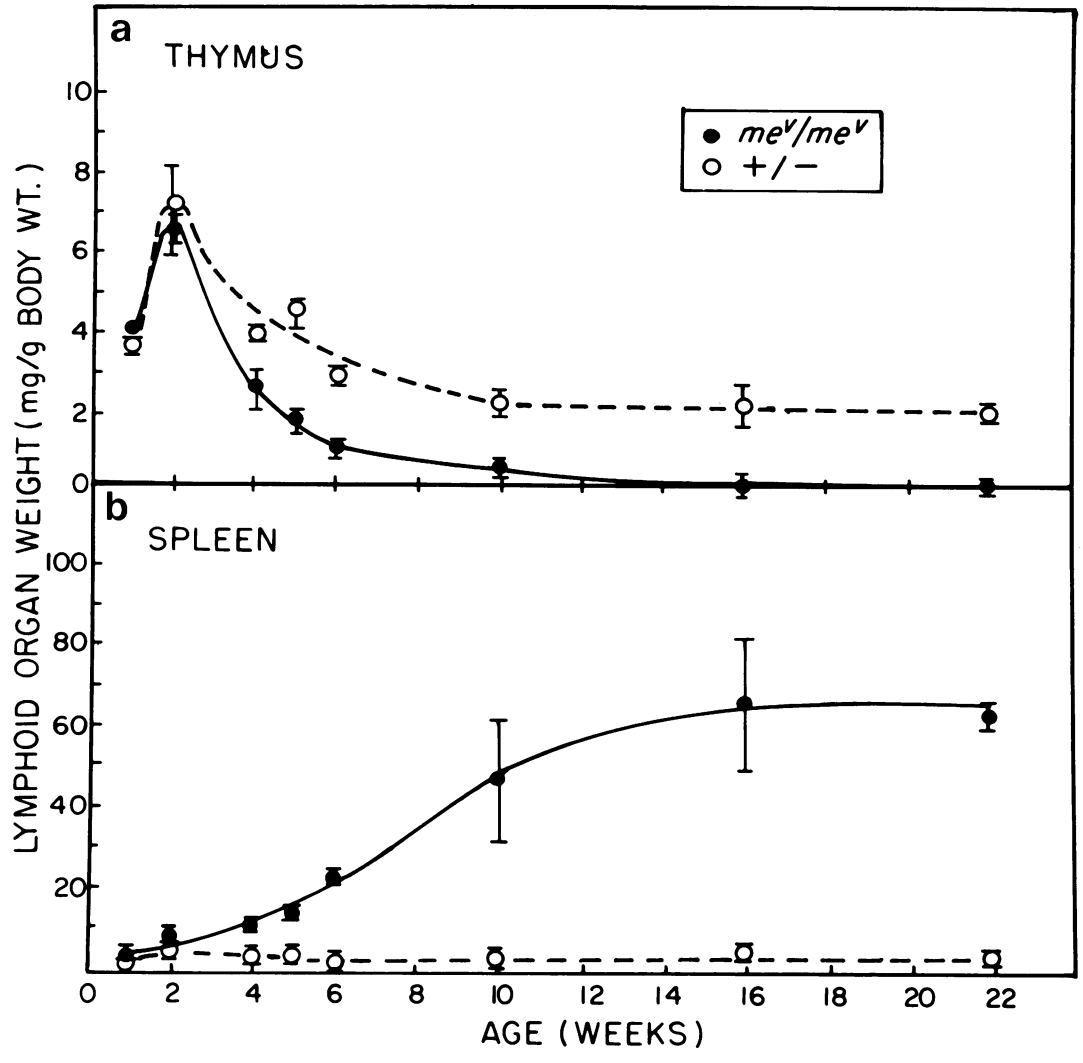

Figure 6—Lymphoid organ to body weight ratio (milligrams per gram body weight) in me^v/me^v and littermate +/− mice. Each point represents the mean and standard error of values from 2–7 mice.

dependent on normal testicular androgen production,[16] we analyzed serum testosterone in eleven pairs of me^v/me^v and littermate control males aged 6–15 weeks. The mutant mice showed a significant reduction in serum testosterone, compared with normal littermates (0.85 ± 0.19 ng/ml for me^v/me^v mice versus 3.51 ± 1.06 ng/ml for +/− controls; $P < 0.01$). If the impairment in spermatogenesis were due to low androgen production, it might be expected that administration of testosterone would alleviate the defect. In a preliminary experiment, five male me^v/me^v mice received subcutaneous implants of 0.5 mg testosterone pellets (Innovative Research of America, Rockville, MD) at 3 weeks of age. Although no progeny resulted from pairing these treated males with normal females, histologic sections prepared from the testes of mice treated with testosterone 8–10 weeks earlier revealed complete spermatogenesis with ample numbers of epididymal sperm.

Discussion

The occurrence of the viable motheaten mutation on the same inbred strain as the original mutation at this locus enables a direct comparison of the phenotypic effects of *me* and me^v without variability caused by differences in genetic background. The most striking differences in phenotypic expression of these alleles is the threefold increase in survival of me^v/me^v mice. That compound me/me^v mice have an increased life span similar to that of homozygous me^v/me^v mice indicates that, at least concerning

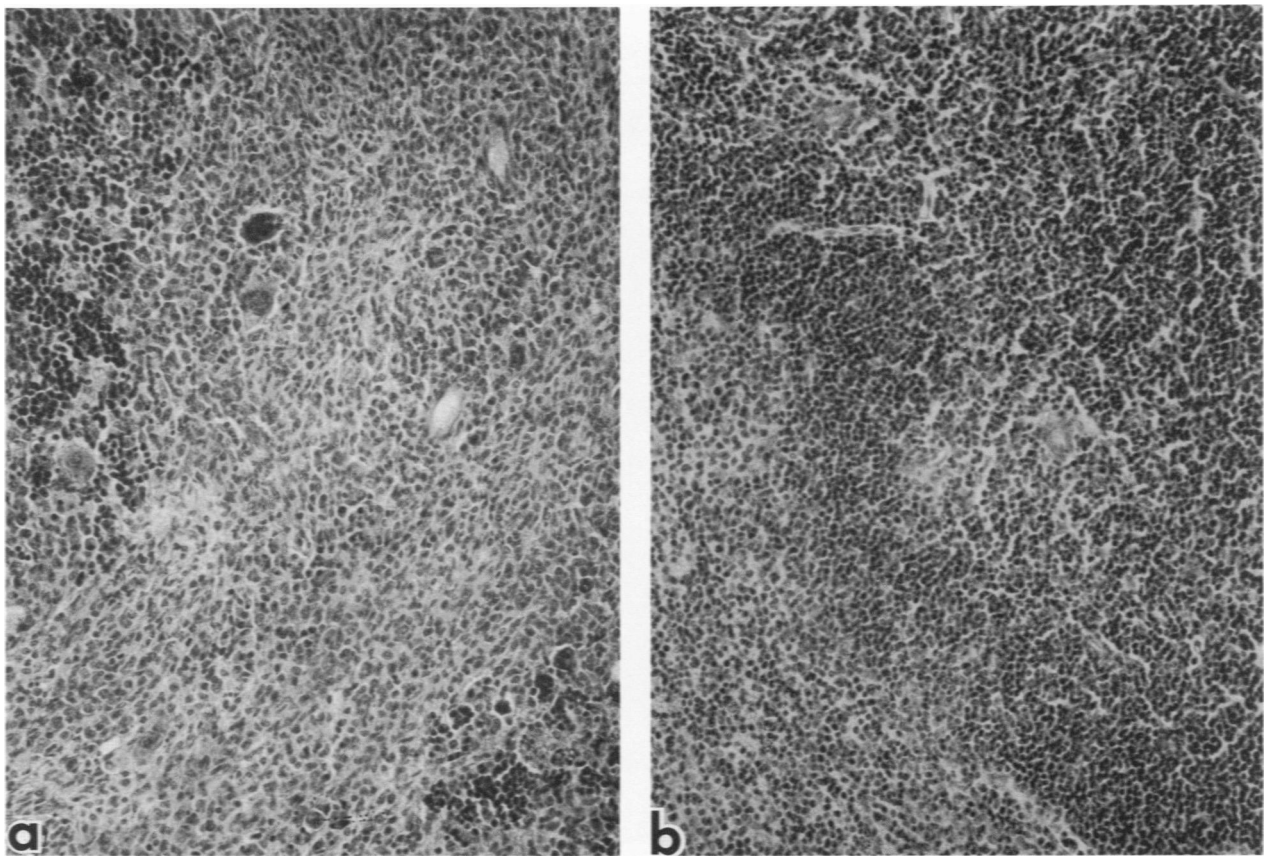

Figure 7 — Spleens from 15-week-old mice. **a** — *me*^{v}/*me*^{v} spleen showing depletion of lymphocytes from a follicle. **b** — Littermate +/− spleen showing normal follicular structure. (H&E, ×150)

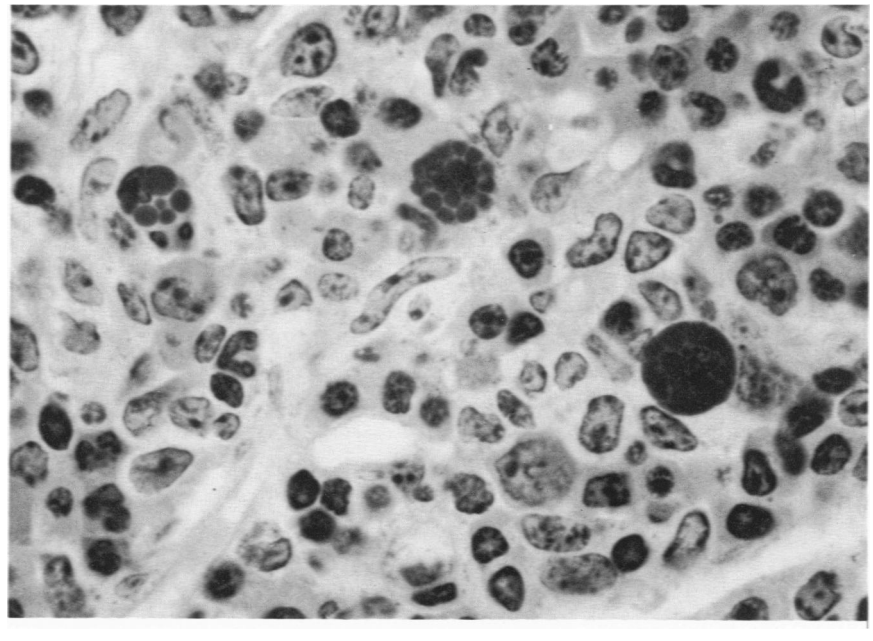

Figure 8 — Plastic-embedded 2-μ section of lymph nodes from a 10-week-old *me*^{v}/*me*^{v} mouse containing atypical plasma cells with Russell bodies. (PAS, ×750)

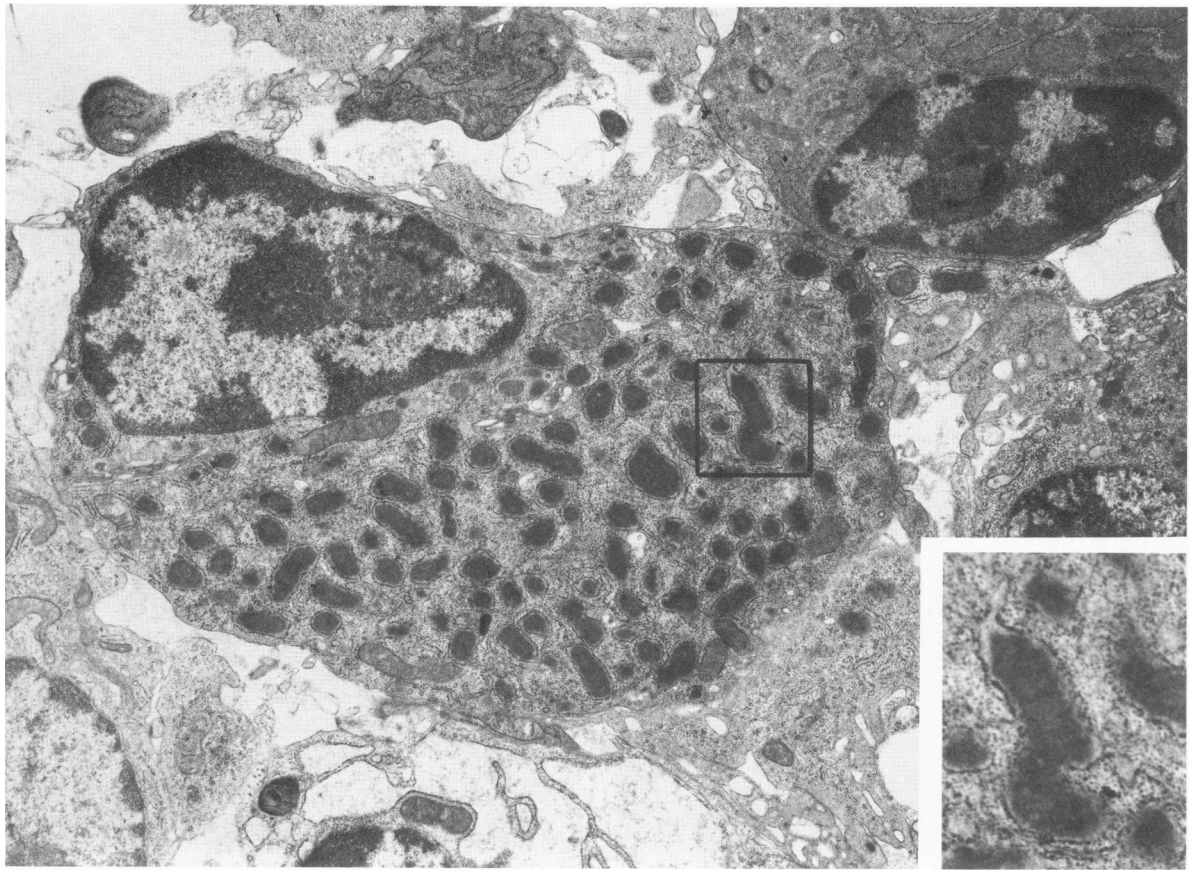

Figure 9 – Electron micrograph of an atypical plasma cell with numerous Russell bodies found in a lymph node from an 8-week-old *me^v/me^v* mouse. (×8700) **Inset** – Continuation of rough endoplasmic reticulum surrounding a Russell body. (×24,000)

survival under conventional mouse room conditions, *me^v* is dominant with regard to *me*. Although the fatal disease process in *me^v/me^v* mice is prolonged, it should be noted that the phenotypic expression of both mutations starts by 4 days of age with the presence of tiny focal aggregates of granulocytes in the skin. While the motheaten mutation results in the rapid development of pneumonitis, the similar pulmonary lesions in *me^v/me^v* mice progress more slowly. The possibility that the delayed development of pneumonitis in *me^v/me^v* mice is due to increased immunocompetence is unlikely, because these mice, like *me/me* mice, have severe deficiencies in humoral and cell-mediated immune function, as well as in endogenous and inducible natural killer cell activity (manuscript in preparation).

Although the pneumonitis in *me^v/me^v* mice progresses more slowly than in *me/me* mice, the eventual histologic appearance of the lungs is strikingly similar in these mutants. The pneumonitis in 3–5-week-old *me/me* or 8–10-week-old *me^v/me^v* mice consists largely of macrophages containing nonbirefringent crystalline-appearing eosinophilic material. Previous studies of the nature of these crystals in *me/me* mice indicated that they were formed within the macrophages and did not result from phagocytosis of preformed crystals.[17] Our observation that extravasation of erythrocytes within alveoli of *me/me* and *me^v/me^v* mice preceded the appearance of crystals within macrophages suggests that the crystals may be associated with erythrocyte degradation. Destruction of erythrocytes is confirmed by the large amount of hemosiderin found within alveolar macrophages. A crystalline material morphologically indistinguishable from that seen within alveolar macrophages of *me^v/me^v* mice has been reported to result from hemoglobin breakdown following uptake of damaged erythrocytes by macrophages. This material, termed hematoidin, was first described by Virchow in 1847 as extracellular crystals found in old hemorrhagic foci.[18] It has also been described in mice 7 days after subcutaneous injection with whole mouse blood[19] or with hemoglobin.[20] Although hematoidin is normally metabolized by the liver after transfer into the blood, its re-

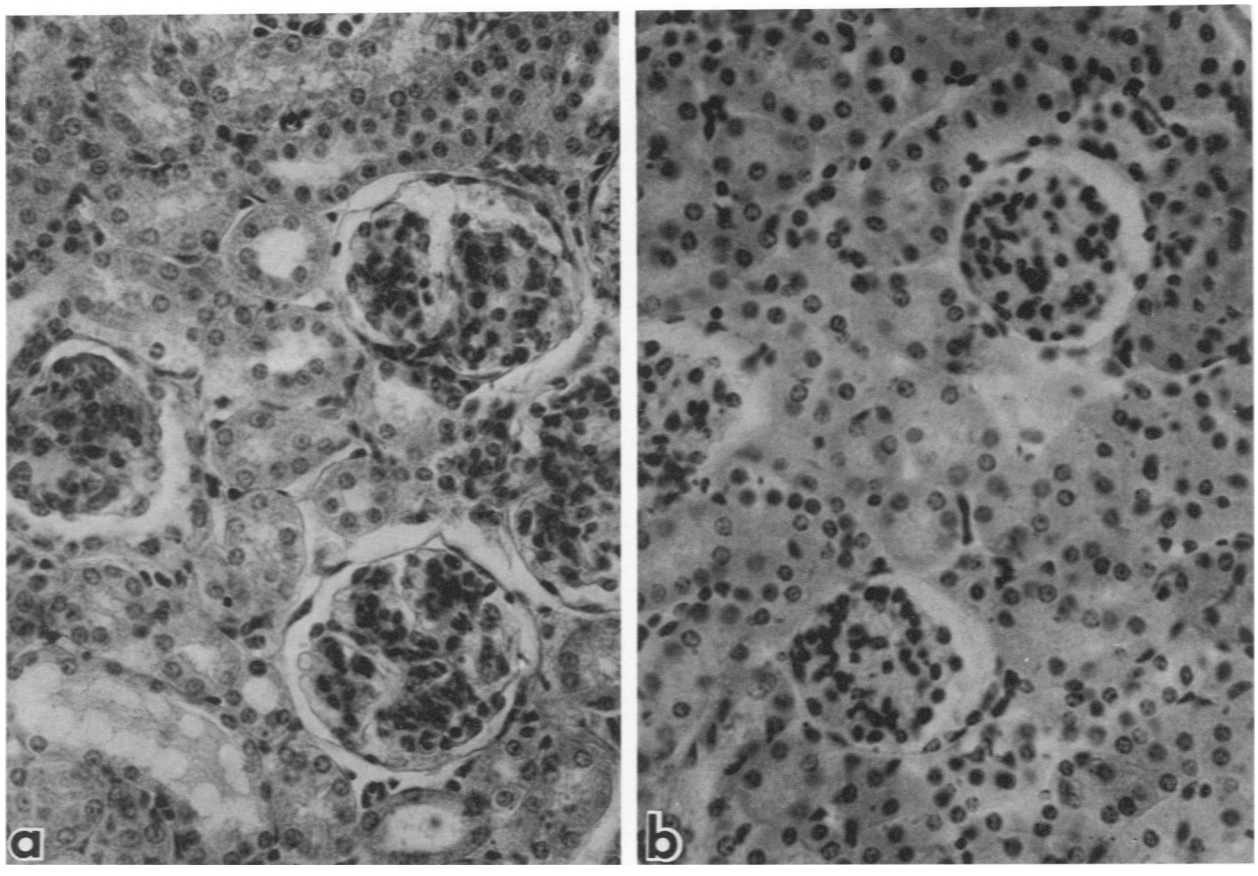

Figure 10 – Kidneys from 20-week-old mice. **a** – *me^v/me^v* kidney with glomerulonephritis. **b** – A +/– kidney showing normal glomerular structure. (H&E, ×300)

moval from hemorrhagic foci can be blocked.[21] It is possible that impaired alveolar macrophage function may contribute to the accumulation of this material in lungs of *me/me* and *me^v/me^v* mice.

Abnormalities were found in all lymphoid tissues of *me^v/me^v* mice. Depletion of cells from the thymic cortex starting at about 3 weeks is followed by necrosis and atrophy by 10 weeks. Since the onset and severity of thymic changes in *me^v/me^v* mice do not differ markedly from those found in *me/me* mice,[8] it is unlikely that the increased longevity of *me^v/me^v* mice is associated with improved thymic function. Moreover, *me^v/me^v* mice lack T-cell function (manuscript in preparation). The absence of follicles in lymph nodes and depletion of lymphocytes from the white pulp of the spleen in this mutant are similar to the histologic changes seen in *me/me* mice.[8] Although atypical plasma cells with Russell bodies have not been previously reported in lymphoid tissues from the *me/me* mutant, a retrospective analysis of PAS-stained sections of lymph nodes from *me/me* mice aged 3–6 weeks revealed the presence of plasma cells with Russell bodies by 4 weeks (unpublished data). Plasma cells containing Russell bodies have been described in human lymphoid malignancies[22] as well as in a variety of human autoimmune diseases, including systemic lupus erythematosus,[23] ulcerative colitis,[24] gastritis, and Hashimoto's thyroiditis.[25] Lymphoid tissues from old NZB mice also contain plasma cells with Russell bodies.[26] These inclusions may result from chronic antigenic stimulation accompanied by a defect in immunoglobulin secretion. As will be reported elsewhere (manuscript in preparation), Russell bodies in plasma cells from *me^v/me^v* mice are reactive with antiimmunoglobulin antisera as determined by both immunofluorescence microscopy and electron microscopy using protein-A gold localization techniques.

Elevated erythropoiesis and myelopoiesis in spleens of *me^v/me^v* mice result in a 10- to 15-fold increase (relative to +/– littermate control mice) in the spleen to body weight ratio by 15 weeks of age. This is accompanied by marked depletion of the white pulp. While previous studies with *me/me* mice showed nor-

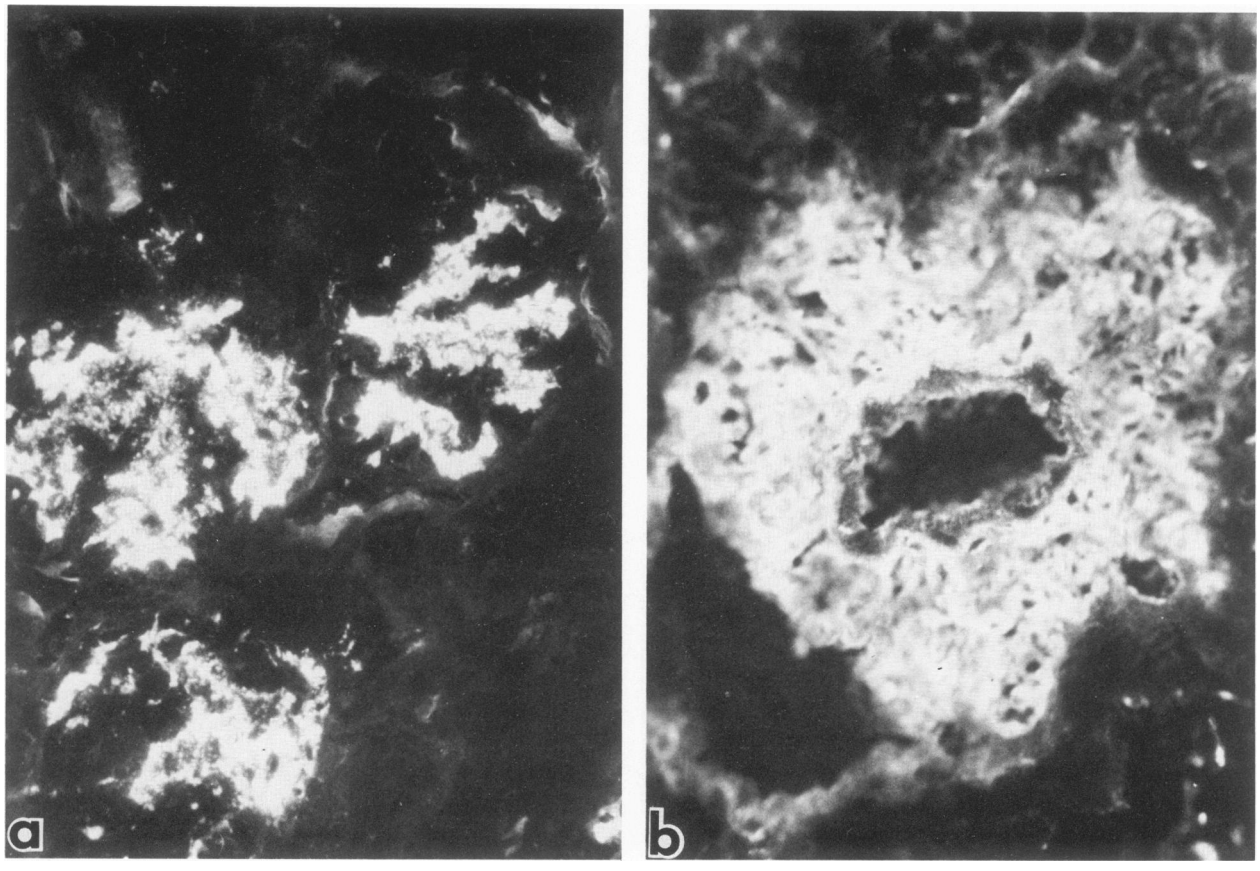

Figure 11 – Frozen sections of tissues from a 10-week-old *me^v/me^v* mouse. **a** – Kidney incubated with fluorescein-conjugated goat antiserum to C3. **b** – Lung incubated with fluorescein-conjugated goat antiserum to IgM. (×1000)

mal erythrocyte numbers, *me^v/me^v* mice develop a severe macrocytic anemia after 9 weeks of age. Concomitant with the development of anemia is a 4-fold increase in the percentage of reticulocytes. As in *me/me* mice,[8] there is an increased level of myelopoiesis in the bone marrow, and the spleen appears to have enhanced erythrocyte production. The finding of hemagglutinating antibodies in plasma of *me^v/me^v* mice (unpublished data) suggests that autoimmunity may play a major role in the development of anemia. Such antierythrocyte autoantibodies have been implicated in the development of anemia in other autoimmune strains of mice.[27] Alternatively, the viable motheaten mutation might result in an intrinsic erythrocyte defect that stimulates the development of autoantibodies.

Sterility in male *me^v/me^v* mice is associated with decreased numbers of Leydig cells and reduced levels of testosterone. Although we have observed neutrophil infiltration between the testicular tubules at 1–2 weeks of age, we have no evidence that the Leydig cell depletion is due to autoimmunity. Impaired spermatogenesis appears to be a consequence of low testosterone levels, since testosterone implants resulted in the production of normal-appearing spermatids. Preliminary experiments to produce progeny from hormone-treated mice mated with normal females have not been successful, however. In addition to causing impaired spermatogenesis, the low testosterone levels in male *me^v/me^v* mice might promote the development of autoimmunity, because prepubertal castration of NZB/NZW F_1 mice results in an earlier appearance of autoantibodies.[28,29] Moreover, androgen therapy prolongs the survival of certain autoimmune strains of mice.[28–30]

In *me^v/me^v* mice, glomerulonephritis is found by 10 weeks of age, and elevated BUN levels are evident in surviving mice by 15 weeks. Although immune complexes were also found in kidneys of very young *me/me* mice,[3] the glomerulonephritis in older *me^v/me^v* mice is more severe. We do not know the underlying basis for the phenotypic differences between *me* and *me^v*, but bone marrow transfer experiments suggest that the increased survival of *me^v/me^v* mice

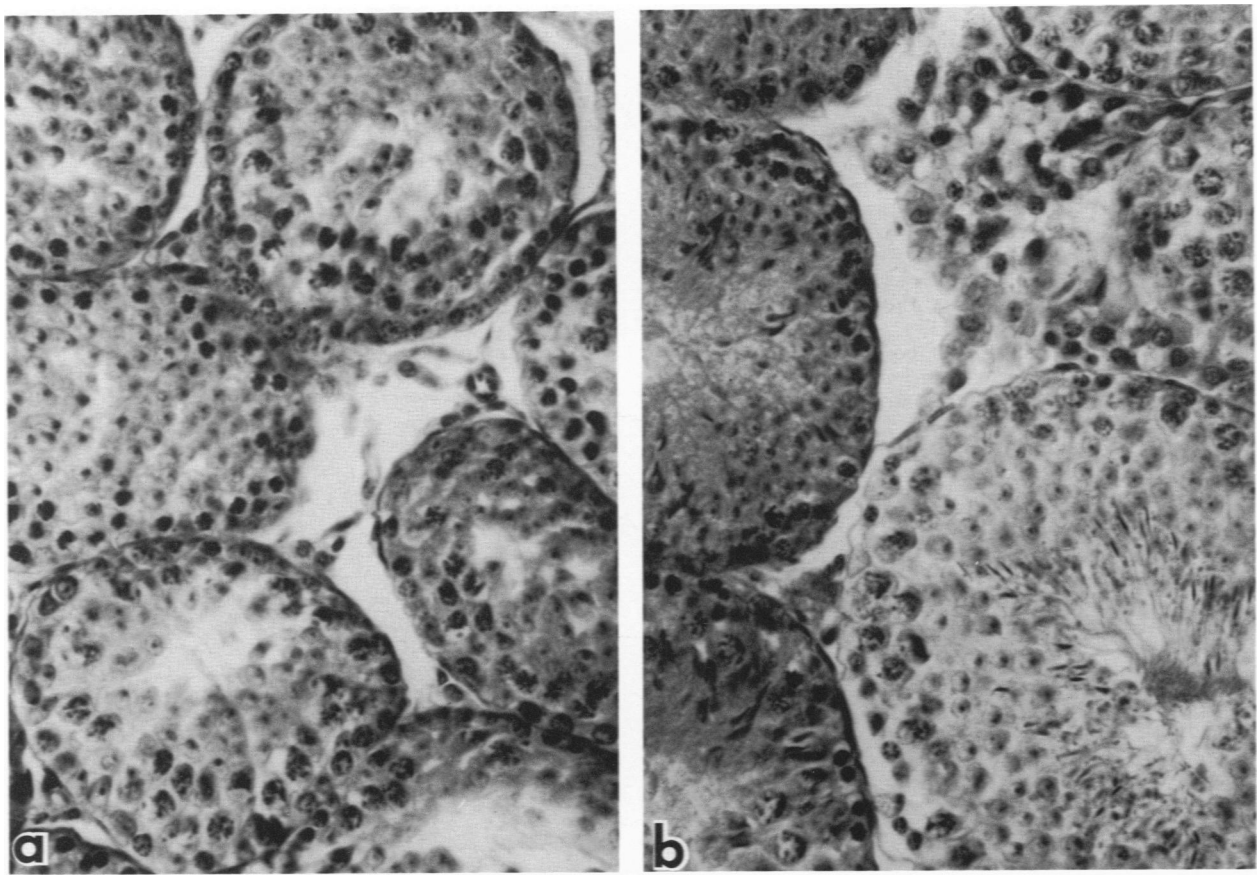

Figure 12—Testes from 10-week-old mice. **a**—*me^v/me^v* testes showing Leydig cell depletion and absence of mature spermatids. **b**—Littermate +/− testes showing normal structure. (H&E, ×300)

compared with *me/me* mice may be due to processes determined by descendants of progenitor cells from the bone marrow. For instance, in a recent study, we found that lethally irradiated syngeneic +/+ recipients of bone marrow cells from *me/me* mice die from acute pulmonary hemorrhage 2–3 weeks after injection[31]; also, preliminary experiments reveal that lethally irradiated syngeneic +/+ recipients of bone marrow from *me^v/me^v* mice have a mean survival time of 8 weeks after injection. Moreover, these recipients develop a chronic pulmonary pneumonitis similar to that seen in *me^v/me^v* mice (unpublished data). In summary, homozygosity for the viable motheaten mutation results in pathologic abnormalities similar to those previously reported in *me/me* mice. However, the threefold increase in average life span of *me^v/me^v* mice appears to result from a more chronic disease process than is seen in *me/me* mice. The development and progression of the disease are thus more amenable to investigation. Identification of aberrant products of the *me* and *me^v* alleles and the function of the normal allele at the motheaten locus will contribute to knowledge of mammalian immunopathologic mechanisms.

References

1. Shultz LD: Mutant genes affecting development of the immune system: Mouse, Inbred and Genetically Defined strains of Laboratory Animals. Part 1. Mouse and Rat. Edited by PL Altman, DD Katz. Federation of American Societies for Experimental Biology Press, Bethesda, Md, 1979, pp 67–70
2. Gershwin ME, Merchant B: Immunologic Defects in Laboratory Animals. New York, Plenum Press, 1981
3. Shultz LD, Green MC: Motheaten, an immunodeficient mutant of the mouse. II. Depressed immune function and elevated serum immunoglobulins. J Immunol 1976; 116:936–943
4. Sidman CL, Shultz LD, Unanue ER: The mouse mutant "motheaten." II. Functional studies of the immune system. J Immunol 1978, 121:2399–2404
5. Davidson WF, Morse HC III, Sharrow SO, Chused TM: Phenotypic and functional effects of the motheaten gene on murine B and T lymphocytes. J Immunol 1979, 122:884–891
6. Clark EA, Shultz LD, Pollack SB: Mutations in mice that influence natural killer (NK) cell activity. Immunogenetics 1981, 12:601–613

7. Shultz LD, Zurier RB: "Motheaten," a single gene model for stem cell dysfunction and early onset autoimmunity, Genetic Control of Autoimmune Disease. Edited by NR Rose, PE Bigazzi, NL Warner. Amsterdam, Elsevier/North Holland, 1978, pp 229–240
8. Green MC, Shultz LD: Motheaten, an immunodeficient mutant of the mouse. I. Genetics and pathology. J Hered 1975, 66:250–258
9. Lillie RD: Histopathology Technic and Practical Histochemistry. New York, Blakiston, 1954
10. Geissler EN, McFarland EC, Russell ES: Analysis of pleiotropism at the dominant white spotting (W) locus of the house mouse: A description of ten new W alleles. Genetics 1981, 97:336–361
11. Geissler EN, Russell ES: Analysis of the hematopoietic effects of new dominant spotting (W) mutations of the mouse: I. Influence upon hematopoietic stem cells. Exp Hematol 1983, 11:452–460
12. Dunn TB: Normal and pathological anatomy of the reticular tissue in laboratory mice with a classification and discussion of neoplasms. J Natl Cancer Inst 1954, 14:1281–1433
13. Yam LT, Li CY, Crosby WH: Cytochemical identification of monocytes and granulocytes. Am J Clin Pathol 1971, 55:283–290
14. Lucas AM, Abraham GE: Radioimmunoassay of testosterone in murine plasma. Anal Lett 1972, 5:773–783
15. Russell W: An address on a characteristic organism of cancer. Br Med J 1890, 2:1356–1360
16. Steinberger E: Hormonal control of spermatogenesis, Endocrinology. Vol 3. Edited by LJ Degroot, GF Cahill Jr, WD Odell, L Martini, JT Potts Jr, DH Nelson, E Steinberger, AI Winnegrad. New York, Grune and Stratton, 1979, pp 122–123
17. Ward JM: Pulmonary pathology of the motheaten mouse. Vet Pathol 1978, 15:170–178
18. Virchow R: Die Pathologischen pigmente. Virchows Arch 1847, 1:379–404
19. Niven JSF: The formation of hematoidin *in vitro* from mammalian erythrocytes. J Pathol 1935, 41:177–182
20. Muir R, Niven JSF: The local formation of blood pigments. J Pathol 1935, 41:183–197
21. Pearse AG: Histochemistry. Theoretical and Applied. New York, Brown and Company, 1960, pp 657–658
22. Blum J, Bendt M, Wilk A: A study of Russell bodies in human monoclonal plasma cells by means of immunofluorescence and electron microscopy. Acta Pathol Microbiol Scand [A] 1976, 84:335–349
23. Arno J: Atlas of Lymph Node Pathology. Philadelphia, J.B. Lippincott, 1980, p 37
24. Gebbers J-O, Otto HF: Plasma cell alterations in ulcerative colitis: An electron microscopic study. Pathol Eur 1976, 11:271–279
25. Hsu SM, Hsu PL, McMillan P, Fanger H: Russell bodies. A light and electron microscopic immunoperoxidase study. Am J Clin Pathol 1982, 77:26–31
26. Vries MJ, Hijmans W: Pathological changes of thymic epithelial cells and autoimmune disease in NZB, NZW, and (NZB × NZW)F_1 mice. Immunology 1967, 12:179–196
27. Heyler BJ, Howie JB: Spontaneous autoimmune disease in NZB/BL mice. Br J Haematol 1963, 9:119–131
28. Roubinian JR, Papoian R, Talal L: Androgenic hormones modulate autoantibody response and improve survival in murine lupus. J Clin Invest 1977, 59:1066–1070
29. Roubinian JR, Talal N, Greenspan JS, Goodman JR, Siiteri PK: Effect of castration and sex hormone treatment on survival, anti-nucleic acid antibodies, and glomerulonephritis in NZB/NZW F_1 mice. J Exp Med 1978, 147:1568–1583
30. Steinberg AD, Roths JB, Murphy ED, Steinberg RT, Raveche E: Effects of thymectomy or androgen administration upon the autoimmune disease of MRL/Mp-*lpr/lpr* mice. J Immunol 1980, 125:871–873
31. Shultz LD, Bailey CL, Coman DR: Hematopoietic stem cell function in motheaten mice. Exp Hematol 1983, 11:667–680

Acknowledgments

We are grateful to Dr. Margaret C. Green and John B. Roths for critically reviewing the manuscript. The skillful technical assistance of Eleanor McFarland, Kathy Shultz, Bonnie Lyons, Ann Higgins, Priscilla Jewett, and Suzie Taylor is gratefully acknowledged. The expert secretarial assistance of Fran Hood is sincerely appreciated.